ELECTRICALLY PUMPED, RELATIVISTIC, FREE ELECTRON WAVE GENERATORS

by

G. Bekefi

Preprint PFC/JA-79-13

Plasma Research Report

PRR 79/21
October 1979

ELECTRICALLY PUMPED, RELATIVISTIC, FREE ELECTRON WAVE GENERATORS

G. Bekefi

Department of Physics and Research Laboratory of Electronics

Massachusetts Institute of Technology

Cambridge, Massachusetts 02139

ABSTRACT

Stimulated scattering induced by the longitudinal electric field of a pump wave is studied theoretically for the case of dense, relativistic electron beams traveling in cylindrical metal waveguides. Two processes are examined. In one, the pump wave decays parametrically into a slow and a fast space charge wave. In the other, it decays into a slow space charge wave and a TM wave of the guide. The frequency characteristics and stimulated growth rates are given for each process, as a function of beam diameter, velocity, and density.

I. INTRODUCTION

Stimulated Compton[1,2,3] or Raman[4-10] scattering in relativistic electron beams has been induced by applying a static, spatially periodic, transverse magnetic field, or by injecting a propagating electromagnetic wave. In either case, the electrons acquire a velocity modulation in a direction transverse to the beam; the longitudinal ponderomotive force (radiation pressure) that develops causes the desired axial bunching of the electrons. The possibility of pumping free electron lasers by means of electric fields rather than by magnetic fields, as is prevalent today, has recently evoked some interest.[11,12,13,14] There exist two rather distinct situations. When the electric field of the pump wave is polarized at <u>right angles</u> to the beam axis, the same physical principles apply as when the system is pumped magnetically: the beam electrons cannot distinguish between the two types of excitation. Thus, in the computations[15-21] of stimulated growth rates, etc., one merely replaces the amplitude $|\vec{B}|$ of the magnetic pump by the amplitude $|\vec{E}|/c$ of the corresponding transverse electric pump.

Conditions are different when the electric field of the pump wave is oriented <u>along</u> the beam axis, which is the subject matter of this paper. Here the oscillating electric field of the pump wave excites axial electron oscillations and beam bunching directly without the need of an "intermediary" ponderomotive force. Two interactions will be considered. In one, the axial electric field of the pump wave decays parametrically into two space charge waves of the beam-filled cylindrical waveguide. This three-wave process is illustrated schematically in the dispersion diagrams of

Fig. 1. The upper diagram represents the interaction as seen by an observer moving axially with the electron velocity (the beam frame), and the lower diagram represents the same interaction as viewed by a stationary observer (the laboratory frame, henceforth labelled L). The three waves are: the pump wave (1). The forward scattered wave (2) propagating antiparallel to the beam electrons. And the back scattered wave (3) which in the laboratory frame is doubly Doppler upshifted in frequency and therefore of interest in microwave and submillimeter wave generation. It is seen that in the laboratory frame one can view the process as a coupling of the slow (negative energy) and fast (positive energy) space charge waves. This coupling has been studied in the past,[11,13] but only in the limit of beams having infinite transverse dimensions, traveling in free space. Indeed, one motivation of this paper is to examine the effects of finite beam geometry and the proximity of the waveguide walls.

In the other interaction studied here, the axial electric pump wave (1) decays into a space charge wave (2) and a TM wave (3) of the cylindrical metal waveguide filled with beam electrons. This is illustrated by the dispersion diagrams shown in Fig. 2. We note that these diagrams are the same as those applicable to magnetically pumped free electron lasers, as they must be, since similar types of waves are operative in both cases (a pump wave, a space charge wave, and an electromagnetic wave). But, there is one proviso. In a magnetically pumped system, the pump wave may decay into either a TM or TE wave. But in the presence of an axial electric pump, the interaction can proceed via a TM mode only, because it alone possesses the axial electric field neces-

sary for electron bunching. Needless to say, the stimulated growth rates in the two systems are very different, even though they may have the same dispersion diagrams.

Figures 1 and 2 have been drawn such that in laboratory frame of reference, the pump wave has a finite wave number but zero frequency. These then represent special cases of static, spatially periodic electric pumps. We stress that the results of Section II below are not restricted to this case alone. They are equally applicable to pumps having nonzero frequency, that is, to traveling wave pumps. However, in Sections III and IV, where numerical results are presented, we limit our discussion to static pumps only.

II. DERIVATION OF THE NONLINEAR RATE EQUATIONS

In this section we derive the nonlinear rate equations governing the temporal growth (or decay) of the wave amplitudes propagating on the electron beam. To this purpose we first obtain the appropriate nonlinear wave equation. The geometry of the system is illustrated in Fig. 3. A homogeneous electron beam of velocity v_o traveling along the z axis fills uniformly a cylindrical waveguide of radius a. The beam is subjected to a uniform, axial magnetic field B_{oz} so strong that all electron motions (steady and oscillatory) can be considered purely axial, such that $\vec{v}=\hat{z}\, v_z$.

The electron thermal velocities are neglected (cold plasma approximation), thus permitting use of fluid equations in describing the beam kinetics. In the beam frame of reference in which the computations will, henceforth, be performed (all Lorentz

transformations to the laboratory (L) frame can be made later, as needed), the particle and momentum conservation equations take the form

$$\frac{\partial n}{\partial t} + N \frac{\partial v_z}{\partial z} = - \frac{\partial}{\partial z} (nv_z) \tag{1}$$

$$\frac{\partial v_z}{\partial t} - \frac{q}{m_o} E_z = - v_z \frac{\partial v_z}{\partial z} \tag{2}$$

Here q and m_o are the electron charge and rest mass, respectively; n is the perturbed rf electron beam density, and N is the steady state average density; v is the perturbed rf velocity (v_o=0 in this frame), and E_z is the z component of the rf field. For convenience all nonlinear terms have been relegated to the right-hand sides of Eqs. (1) and (2).

The above equations are to be solved in conjunction with Maxwell's equations,

$$\nabla \cdot \vec{E} = \frac{q}{\epsilon_o} n \tag{3}$$

$$\nabla \times \vec{B} = \mu_o \epsilon_o \frac{\partial \vec{E}}{\partial t} + \mu_o \vec{J} \tag{4}$$

$$\nabla \times \vec{E} = - \frac{\partial \vec{B}}{\partial t} \tag{5}$$

$$\nabla \cdot \vec{B} = 0 \tag{6}$$

with

$$\vec{J} = \hat{z} q (N v_z + n v_z) \tag{7}$$

as the rf current, composed of a linear and nonlinear part. In the presence of the large axial magnetic field, the TM and TE waveguide modes are uncoupled,[22] but only the former will be of interest here since they possess the requisite axial electric field E_z (see Section I). With this in mind, we eliminate $\vec{B}$ from Eqs. (4) and (5) and using Eq. (3) obtain for the z component of

electric field,

$$\nabla^2 E_z - \frac{q}{\varepsilon_o}\frac{\partial n}{\partial z} = \mu_o \varepsilon_o \frac{\partial^2 E_z}{\partial t^2} + \mu_o \frac{\partial J_z}{\partial t} \tag{8}$$

(Once E_z is known, the remaining field components E_r, E_θ, B_r, and B_θ are deduced from Eqs. (5) and (6).) On substituting Eq. (7) in Eq. (8), differentiating twice with respect to time, and eliminating $\partial n/\partial t$ and $\partial v/\partial t$ with the aid of Eqs. (1) and (2), we arrive at the sought-after nonlinear wave equation,

$$\frac{\partial^2}{\partial t^2}\nabla_\perp^2 E_z + \left(\omega_p^2 + \frac{\partial^2}{\partial t^2}\right)\bigcirc E_z = \frac{m_o}{q}\omega_p^2 \bigcirc \left[v_z \frac{\partial v_z}{\partial z} - \frac{\partial}{\partial t}\left\{\frac{n v_z}{N}\right\}\right] \tag{9}$$

which, in conjunction with Eqs. (1) and (2), will be used as a starting point in calculating the rate equations. In Eq. (9), $\omega_p \equiv (Ne^2/m_o\varepsilon_o)^{1/2}$ is the plasma frequency,

$$\nabla_\perp^2 = \frac{1}{r}\frac{\partial}{\partial r}\left[r\frac{\partial}{\partial r}\right] + \frac{1}{r^2}\frac{\partial^2}{\partial \theta^2} \tag{10}$$

is the transverse Laplacian operator, and

$$\bigcirc = \frac{\partial^2}{\partial z^2} - \frac{1}{c^2}\frac{\partial^2}{\partial t^2} \tag{11}$$

is a wave propagation operator which, in the quasi-static approximation (usually applicable to the slow space charge waves), reduces to $\bigcirc = \partial^2/\partial z^2$. The nonlinear terms situated on the right-hand side of Eq. (9) are easily recognized: $v_z \partial v_z/\partial z$ is the nonlinear term appearing in momentum conservation Eq. (2); and nv_z is the nonlinear current density appearing in Eq. (1).

In the absence of nonlinear phenomena, the solution of Eq. (9) is given by the familiar result[22,23]

$$E_z = E_o J_m (p_{m\nu} r/a) e^{j(\omega t + m\theta + kz)} \tag{12}$$

where E_o is the constant field amplitude, J_m is the Besel function

of order m and $p_{m\nu}$ is the νth zero of the mth order Bessel function. The frequency ω and wavenumber k are related through a dispersion equation which has two branches. A high frequency branch,

$$k^2a^2 = \left(\frac{\omega a}{c}\right)^2 - p_{m\nu}^2 \frac{\omega^2}{\omega^2-\omega_p^2} \qquad \text{for } \omega \gtrsim \omega_c \tag{13}$$

which represents the TM electromagnetic waveguide modes perturbed by the presence of the electron beam (one of these is shown in the upper part of Fig. 2a). This infinite set of modes exists only at frequencies ω exceeding certain cutoff frequencies ω_c given by $\omega \gtrsim \omega_c \equiv [(p_{m\nu}c/a)^2+\omega_p^2]^{1/2}$. And then there is the low frequency branch

$$k^2a^2 = \left(\frac{\omega a}{c}\right)^2 + p_{m\nu} \frac{\omega^2}{\omega_p^2-\omega^2} \qquad \text{for } \omega \lesssim \omega_p \tag{14}$$

which extends from $\omega=0$ to $\omega=\omega_p$, and represents the space charge waves (one of this infinite set of waves is shown in Fig. 1 and also as the lower branch of Fig. 2).

To solve the nonlinear wave Eq. (9), in conjunction with Eqs. (1) and (2), we write E_z, v_z, and n as a sum of three terms representing the three interacting waves, namely

$$\left.\begin{aligned} E_z &= \frac{1}{2} \sum_{\ell=1,2,3} E_{o\ell}(t) J_m(p_{m\nu}r/a) e^{j\psi_\ell} + \frac{1}{2} \sum_{\ell=1,2,3} \text{C.C.} \\ v_z &= \frac{1}{2} \sum_{\ell=1,2,3} V_\ell(t) e^{j\psi_\ell} + \frac{1}{2} \sum_{\ell=1,2,3} \text{C.C.} \\ n &= \frac{1}{2} \sum_{\ell=1,2,3} N_\ell(t) e^{j\psi_\ell} + \frac{1}{2} \sum_{\ell=1,2,3} \text{C.C.} \end{aligned}\right\} \tag{15}$$

Here $E_{o\ell}(t)$, $V_\ell(t)$ and $N_\ell(t)$ are complex amplitudes that vary slowly with time, and Ψ_ℓ are the phases given by

$$\psi_\ell = \omega_\ell t + m_\ell \theta + k_\ell z \qquad (\ell = 1, 2, 3). \tag{16}$$

To proceed with the problem, we substitute Eqs. (15) in Eq. (9) and equate terms on the left-hand side of Eq. (9) that have phase ψ_1 to terms on the right-hand side that have the same phase $\psi_1 = \psi_2 + \psi_3$; and similarly for ψ_2 and ψ_3. In this way[24] we are, in fact, invoking exact phase matching which is synonymous to the requirement that the "selection rules"

$$\begin{aligned} \omega_1 &= \omega_2 + \omega_3 \\ \vec{k}_1 &= \vec{k}_2 + \vec{k}_3 \\ m_1 &= m_2 + m_3 \end{aligned} \tag{17}$$

be obeyed. The remaining terms that do not obey Eqs. (17) are nonresonant and they do not contribute to the three-way processes considered. Under the assumption of a constant amplitude pump wave (wave 1), the aforementioned manipulations result in two coupled equations for the amplitude growth rates of the forward and backward scattered waves 2 and 3 respectively. We also assume, for the sake of simplicity, that the waves are excited in the same waveguide mode (m,ν) and thus obtain the following rate equations,

$$\frac{\partial E_{02}}{\partial t} = \frac{q}{4m_0} E_{01}\, E^*_{03} \left(\frac{\omega_2^2}{\omega_1\omega_3}\right)\left(\frac{k_1}{\omega_1} + \frac{k_2}{\omega_2} + \frac{k_3}{\omega_3}\right)\left[1 - \left(\frac{\omega_2}{k_2 c}\right)^2\right]\left[1 - \left(\frac{\omega_2}{k_2 c}\,\frac{\omega_2}{\omega_p}\right)^2\right]^{-1}$$

$$\frac{\partial E_{03}}{\partial t} = \frac{q}{4m_0} E_{01}\, E^*_{02} \left(\frac{\omega_3^2}{\omega_1\omega_2}\right)\left(\frac{k_1}{\omega_1} + \frac{k_2}{\omega_2} + \frac{k_3}{\omega_3}\right)\left[1 - \left(\frac{\omega_3}{k_3 c}\right)^2\right]\left[1 - \left(\frac{\omega_3}{k_3 c}\,\frac{\omega_3}{\omega_p}\right)^2\right]^{-1} \tag{18}$$

We see from Eqs. (18) that both the backward and forward scattered waves grow exponentially with time. Setting E_{02} and E_{03} proportional to $\exp(\Gamma t)$ and solving Eqs. (18) simultaneously

we obtain for the temporal grow rate Γ the result,

$$\Gamma = \frac{q}{m_o} \frac{E_{1z}}{v_o} G \tag{19}$$

Here E_{01} is the amplitude of the pump wave, v_o is the beam velocity and G, a dimensionless quantity, is a function of the beam parameters and the dispersion characteristics of all three interacting waves. It is given by

$$G = \frac{1}{4} \left(\frac{\omega_2 \omega_3}{\omega_1^2}\right)^{1/2} \left(\frac{v_o}{v_1} + \frac{v_o}{v_2} + \frac{v_o}{v_3}\right) \times \left\{ \left[1 - \frac{v_2^2}{c^2}\right]\left[1 - \frac{v_3^2}{c^2}\right]\left[1 - \frac{v_2^2}{c^2}\frac{\omega_2^2}{\omega_p^2}\right]^{-1}\left[1 - \frac{v_3^2}{c^2}\frac{\omega_3^2}{\omega_p^2}\right]^{-1} \right\}^{1/2} \tag{20}$$

with $v_1 = \omega_1/k_1$, $v_2 = \omega_2/k_2$, and $v_3 = \omega_3/k_3$, as the wave velocities.

The above equations refer to either of the two processes illustrated in Figs. 1 and 2. The frequency ω is related to the wave number k of each wave through the linear dispersion equation applicable to that wave. Moreover, all ω's and k's must satisfy the selection rules of Eqs. (17). Inserting these requirements in Eqs. (19) and (20) yields the stimulated growth rate for the interaction in question. In Section III we do this for the case of the two interacting space charge waves (Fig. 1); and in Section IV we do the same for the interaction of the space charge wave with the TM electromagnetic wave (Fig. 2).

III. ELECTRIC FIELD PUMPING OF THE SLOW AND FAST SPACE CHARGE WAVES

Here we consider the pumping of two space charge waves (Fig. 1) by a static electric pump having a spatial periodicity in the laboratory frame equal to $\ell_L=2\pi/k_{1L}$. From the Lorentz transformations

$$\begin{aligned} \omega &= \gamma(\omega_L + \beta c k_L) \\ k &= \gamma(k_L + \beta\omega_L/c) \end{aligned} \tag{21}$$

and the fact that $\omega_{1L}=0$, it follows that the pump wave obeys the dispersion equation in the beam frame

$$k_1 = \omega_1/\beta c = \omega_1/v_o \tag{22}$$

with $k_1=\gamma k_{1L}=2\pi\gamma/\ell_L$, $\beta=v_o/c$, and $\gamma=\{1-(v_o/c)^2\}^{-1/2}$.

The two space charge waves must satisfy relation (14). If, as is very often the case, $(\omega_p a/cp_{m\nu})^2<<1$, which states that the square of the phase velocity be much less than c^2, the first term on the right-hand side of Eq. (14) can be neglected. We shall do so here and obtain for waves (2) and (3) the simpler dispersion law,

$$(k_{2,3}a)^2 = p_{m\nu}^2 \frac{\omega_{2,3}^2}{\omega_p^2-\omega_{2,3}^2} \tag{23}$$

The selection rules given by Eqs. (17) together with Eqs. (22) and (23), fully determine the frequencies ω_2 and ω_3 in terms of the pump frequency ω_1, (and they likewise determine k_2 and k_3 in terms of k_1). The results of the calculations are illustrated in Fig. 4. It shows plots of ω_2/ω_1 and ω_3/ω_1, as a function of beam parameters, specified by the quantity $b\equiv(a\omega_p/v_o p_{m\nu})$; (b equals the ratio of the maximum phase velocity of the space

charge wave to the beam velocity, v_o). Each curve is for a different value of the normalized pump frequency ω_1/ω_p.

Suppose b, and thus the beam parameters, are fixed. Then, as the pump frequency ω_1 is increased from zero to its maximum allowable value $\omega_1=2\omega_p$, the two scattered waves approach $\omega_2=\omega_3=\omega_p$, and $\omega_1=2\omega_3$. This is reminiscent[13,25,26] of parametric amplifiers in which the pump drives the system at twice the "signal" frequency. We shall show momentarily that under these conditions, the maximum growth rate is achieved. We note that in our system however, pumping at <u>twice</u> the signal frequency can occur only for one value of ω_1, namely $\omega_1=2\omega_p$. This restriction on the pump frequency comes about because we excite the beam with a static pump wave. When one pumps with traveling waves[25,26] selection rules (17) allow ω_1 to take on a large variety of other values.

To compute the growth rate of the two participating space charge waves we note that generally their phase velocities are much less than the speed of light c. Consequently, the term in the curly {} brackets of Eq. (20) approaches unity. In this "quasi-static approximation" used here

$$G \simeq \frac{1}{4}\left(\frac{\omega_2\omega_3}{\omega_1^2}\right)^{1/2}\left(\frac{v_o}{v_1}+\frac{v_o}{v_2}+\frac{v_o}{v_3}\right) \qquad (24)$$

Figure 5 shows a plot of G as a function of the beam parameter $b=(a\omega_p/v_o p_{m\nu})$, for different values of the normalized pump frequency ω_1/ω_p. It is noteworthy that when $1<\omega_1/\omega_p\leq 2$ the gain factor is almost independent of b, and is thus almost independent of the beam cross section a. This is a most satisfying result. In the limit of "thin" and "thick" beams one then finds that

for thin beams:

$$G(b\to 0) = \frac{1}{16}[2 + \alpha^2] \qquad (0\lesssim\alpha\lesssim 2) \tag{25}$$

for thick beams:

$$\begin{aligned} G(b \to \infty) &= [(\alpha^2-1)(\alpha+1)]^{1/2}/4\alpha \qquad (1<\alpha\lesssim 2) \\ &= 0 \qquad\qquad\qquad\qquad\quad (0\lesssim\alpha\lesssim 1) \end{aligned} \tag{26}$$

where $\alpha \equiv \omega_1/\omega_p$.

The maximum value of the growth rate parameter is G=3/8 and occurs when $\alpha=2$ ($\omega_1=2\omega_p$). This gives a temporal growth rate (Eq. (19)) equal to

$$\Gamma(\max) = \frac{3}{8}\left(\frac{q}{m_o}\frac{E_{1z}}{v_o}\right) \tag{27}$$

a result obtained previously[13] in the thick beam limit (E_{1z} is the amplitude of the longitudinal electric field of the pump wave). It is instructive to compare Γ with the growth rate[18] $\Gamma_\perp$ of the free electron Raman laser pumped with a static, spatially periodic transverse electric field $E_{1\perp}$ (or a transverse magnetic field of equivalent strength, $B_{1\perp} = E_{1\perp}/c$):

$$\Gamma_\perp \simeq \frac{1}{2}\left(\frac{\omega_p}{\omega_1}\right)^{1/2}\left(\frac{q}{m_o}\frac{E_{1\perp}}{v_o}\right) \tag{28}$$

Since in these lasers $\omega_1 >> \omega_p$, the associated growth rate is smaller than the expected growth rate obtained for the two interacting space charge waves, in which the pump frequency ω_1 is close to or below $2\omega_p$, as discussed earlier in this section. However, since E_z and $E_\perp$ have different relativistic transformations, comparisons of Γ's are best done in the laboratory frame of reference (see subsection below).

Thermal motion of the beam electrons which causes Landau

damping of the space charge waves, has been neglected throughout the above discussion. Thermal effects impose an upper limit on allowable wave numbers given by $k_3\lambda_D = k_3 v_{th}/\omega_p < 1$ where $\lambda_D = v_{th}/\omega_p$ is the Debye length, and v_{th} is thermal velocity. This inequality restricts the range of beam parameters $b \equiv (a\omega_p/v_o p_{m\nu})$ available to experimentation. In Fig. 6 the "Landau damping limit" D is plotted; it is defined as follows. Let v_{th}/v_o equal the ratio of beam thermal velocity to the beam axial velocity. Then, the inequality

$$D > v_{th}/v_o \tag{29}$$

implies that $k_3 L_D < 1$. We see that Landau damping does not impose very stringent limitations on b except when ω_1/ω_p approaches too closely the value of 2 (when $\omega_1/\omega_p = 2$, $k_3 L_D \to \infty$). We note that for tenuous relativistic electron beams v_{th}/v_o is typically $\lesssim 0.01$, whereas for dense relativistic beams it is $\gtrsim 0.1$.

Transformation to the Laboratory (L) Frame of Reference

In the laboratory frame of reference the gain Γ_L is related to the gain Γ in the beam frame through[17]

$$\Gamma_L = \Gamma\gamma^{-1}[1 + (v_{3g}v_o)/c^2]^{-1} \tag{30}$$

where $v_{3g} = \partial\omega_3/\partial k_3$ is the group velocity of the back scattered wave in the beam frame. Equation (23) gives

$$v_{3g} \simeq \frac{\omega_p a}{p_{m\nu}}\left[1 - \left(\frac{\omega_3}{\omega_p}\right)^2\right]^{3/2} \tag{31}$$

from which it follows that $v_{g3}/c \ll 1$ if, either $(\omega_p a/cp_{m\nu}) \ll 1$ (which is a statement of the quasi-static approximation), or if $(\omega_3/\omega_p) \to 1$. Under these circumstances Γ of Eq. (27) transforms to

$$\Gamma_L(\max) \simeq \frac{3}{8}\left(\frac{q}{m_o}\frac{E_{zL}}{\gamma\beta c}\right) \tag{32}$$

to be compared with $\Gamma_{\perp L}$ of the transversely pumped laser (Eq. (28)):

$$\Gamma_{\perp L} = \left[\frac{\gamma^{1/2}\omega_{po}\ell_L}{32\pi\beta c}\right]^{1/2}\left(\frac{q}{m_o}\frac{E_{\perp L}}{\gamma\beta c}\right) \tag{33}$$

Here $\omega_{po} \equiv (N_L e^2/m_o\varepsilon_o)^{1/2}$. In obtaining the above equations we made use of the following transformations:

$$\begin{aligned} E_z &= E_{zL} \;;\; E_\perp = \gamma E_{\perp L} + \gamma(\vec{v}\times\vec{B})_\perp \\ \omega_1 &= \beta c\gamma k_{1L} \\ &= 2\pi\beta c\gamma/\ell_L \\ \omega_p &= \omega_{pL} \end{aligned} \tag{34}$$

with $\omega_p = (Ne^2/m_o\varepsilon_o)^{1/2}$ and $\omega_{pL} = (N_L e^2/\gamma m_o\varepsilon_o)^{1/2}$; $\omega_{po}=\gamma^{1/2}\omega_{pL}$ is a fictitious plasma frequency without the $\gamma^{1/2}$ factor. However, with this definition of ω_{po}, the γ dependence of the growth rate is exhibited more vividly.

In typical, transversely pumped Raman lasers employing dense relativistic electron beams,[4-10] the term $[\;]^{1/2}$ of Eq. (33) has values in the range from ~0.05 to ~0.5. It has, therefore, a somewhat lower growth rate than the anticipated growth rate of the longitudinally pumped system (Eq. (32)) excited with a field of the same ($E_{zL}=E_{\perp L}$) or equivalent ($E_{zL}=cB_{\perp L}$) strength.

The axial velocity v_o of the beam electrons causes the backscattered wave to be doubly Doppler upshifted, thus making various types of stimulated scattering schemes of potential interest in the generation of millimeter and submillimeter radiation. We have that $\omega_3\approx\omega_p$ and $\omega_1\approx 2\omega_p$, so that $\omega_3\approx\omega_1/2$. Transforming this to the laboratory frame of reference with the help of Eqs. (21) and (34),

yields $\omega_{3L} \simeq k_{1L}\gamma^2\beta c/2$. Thus, the dimensionless quantity F defined by

$$\omega_{3L} = Fk_{1L}\gamma^2\beta c \qquad (35)$$

is useful in making predictions of the expected radiation frequency in terms of γ and the pump periodicity $\ell_L = 2\pi/k_{1L}$. We call F the "frequency enhancement factor". Since ω_3 and k_1 are known in the beam frame, their values are readily transformed into the laboratory frame, and F computed. The results are shown in Fig. 7. We see that F is large for thin beams and small for thick beams so that, for a given γ and ω_p, thin beams give higher frequency waves than thick beams. When $1<\omega_p/\omega_1<2$, F tends asymptotically to a constant value, as the beam thickness is increased. In the limit $b \to \infty$, $F=(1-(\omega_p/\omega_1))$. When $\omega_1/\omega_p=2$, F=0.5, which is a result derived in an earlier publication.[13] For comparison, we note that a beam excited with a transverse, spatially periodic magnetic pump, or a transverse electric pump, has $F_1=(1+\beta)\simeq 2$ as will be shown in the following section.

IV. PUMPING OF THE SLOW SPACE CHARGE WAVE AND A TM WAVEGUIDE MODE

Here we examine the growth of a slow space charge wave and a TM mode of a cylindrical waveguide pumped by a static electric pump. The three participating waves are (see Fig. 2): The pump wave (1) whose dispersion characteristics are given by Eq. (22). The slow space charge wave (2) whose dispersion characteristics are given by Eq. (23), and the fast back-scattered TM wave (3) whose dispersion characteristics are given by Eq. (13). We assume that ω_3 is well above the cutoff frequency ω_c for the mode in ques-

tion, so that $\omega_3/k_3 \approx c$.

Both the pump wave and the back-scattered wave are fast compared with the slow space charge wave. From the first selection rule of Eqs. (17), $\omega_1=\omega_2+\omega_3$, it therefore follows that to good approximation,

$$\omega_3 \simeq \omega_1 \ . \tag{36}$$

Using this result in the second selection rule, $k_1=k_2-k_3$ we find the needed relationship for the ratio v_0/v_2 of beam velocity to the phase velocity of the forward scattered wave (2):

$$(v_0/v_2) \simeq (1+\beta)(\omega_1/\omega_2) \tag{37}$$

Similar ratios for the remaining two waves are:

$$\begin{aligned} (v_0/v_1) &= 1 \\ (v_0/v_3) &= -\beta \end{aligned} \tag{38}$$

Inserting Eqs. (36) through (38) in Eq. (20) for the gain factor G, and noting that $\omega_2 \approx \omega_p$ we obtain

$$\begin{aligned} G &= \frac{1}{4}\left(\frac{\omega_p}{\omega_1}\right)^{1/2}\left[(1-\beta) + (1+\beta)(\omega_1/\omega_p)\right]\{\cdots\}^{1/2} \\ &\simeq \frac{1}{4}(1+\beta)(\omega_1/\omega_p)^{1/2}\{\cdots\}^{1/2} \end{aligned} \tag{39}$$

where the second form of the equation is valid in most cases of interest for which $\beta \to 1$ or $\omega_1/\omega_p >> 1$.

The complicated terms within the curly bracket $\{\cdots\}$ exhibited in Eq. (20) simplify considerably under the assumptions made above. First, for the slow space charge wave (2) we can safely set $(v_2/c)^2=0$. Secondly, using dispersion Eq. (13) for the fast backward scattered wave (3) subject to the condition, ω_3/ω_c, $\omega_3/\omega_p >> 1$, we obtain $\{\cdots\} \simeq (\omega_{co}\omega_p/\omega_3^2)^2$ where $\omega_{co}=(p_{m\nu}c/a)$ is the

cutoff frequency of the (m,ν) mode of the empty cylindrical waveguide. Inserting this result in Eq. (39), it follows that

$$G = \frac{1}{4}(1+\beta)\left(\frac{\omega_p}{\omega_1}\right)^{1/2}\left(\frac{\omega_{co}}{\omega_1}\right) \tag{40}$$

giving the temporal growth rate

$$\Gamma = \frac{1}{4}(1+\beta)\left(\frac{\omega_p}{\omega_1}\right)^{1/2}\left(\frac{\omega_{co}}{\omega_1}\right)\left(\frac{q}{m_o}\frac{E_{1z}}{v_o}\right) . \tag{41}$$

Except for the term (ω_{co}/ω_1), this growth rate is identical with that associated with traversely pumped free electron lasers (see Eq. (28)). The reason for the term (ω_{co}/ω_1) becomes clear when we realize that it originates from the dependence of E_z on frequency. As ω_3 increases relative to the cutoff frequency ω_c, the axial electric field E_z responsible for the interaction decreases proportionately, and vanishes altogether when $\omega_3/\omega_c \to \infty$. Transversely pumped lasers do not require an E_z electric field to achieve bunching (it occurs via $E_\perp$ or $B_\perp$ and the ponderomotive force) and therefore the term ω_{co}/ω_1 is absent from Eq. (28) for $\Gamma_\perp$. Usually $(\omega_{co}/\omega_1)<<1$, and consequently Γ for this type of laser is much smaller than $\Gamma_\perp$ for the transversely pumped laser. This fact will come out even more forceably when we compare the two systems in the laboratory frame of reference later in this section.

Matters are much more favorable for lower frequency operation, near cutoff, $\omega_c/\omega_3 \simeq 1$, in which case E_{3z} has its largest possible value. Now, with $\omega_c/\omega_3 \to 1$, $k_3 \to 0$, $v_o/v_3 = 0$, $v_o/v_2 = \omega_1/\omega_2$, and $v_o/v_1 = 1$. The term in curly brackets in the equation for G becomes $(\omega_p/\omega_3)^2$. Inserting these values in Eqs. (19) and (20) yields

$$G(\omega_3 \simeq \omega_c) \simeq \frac{1}{4}\left(\frac{\omega_p}{\omega_1}\right)^{1/2} \tag{42}$$

and

$$\Gamma(\omega_3 \simeq \omega_c) \simeq \frac{1}{4}\left(\frac{\omega_p}{\omega_1}\right)^{1/2}\left(\frac{q}{m_o}\frac{E_{1z}}{v_o}\right) \tag{43}$$

which, within a factor of 2, is of the same form as the growth rate Γ_1 of the transversely pumped laser (Eq. (28).

Transformation to the Laboratory (L) Frame of Reference

In accordance with Eq. (36), the frequency ω_3 of the back-scattered TM mode is to good approximation equal to the pump frequency ω_1. Transforming this statement to the laboratory reference frame with the aid of Eqs. (21) and (34) yields,

$$\omega_{3L} = k_{1L}\gamma^2\beta c(1+\beta), \quad (k_1 = 2\pi/\ell_L) \tag{44}$$

which exhibits the typical γ^2 frequency multiplication of the pump frequency. A transformation of the growth rate Γ of Eq. (41) gives

$$\Gamma_L = \left[\frac{(1+\beta)^2}{512\pi^3\gamma^{7/2}}\frac{\omega_{po}^2\omega_{co}\ell_L^3}{(\beta c)^3}\right]^{1/2}\left(\frac{q}{m_o}\frac{E_{zL}}{\gamma\beta c}\right) \tag{45}$$

where $\omega_{po}=(N_L e^2/m_o\varepsilon_o)^{1/2}$ and $\omega_{co}=(p_{m\nu}c/a)$.

It is instructive to compare the growth rates of the longitudinally pumped TM mode laser (Eq. (45) with the transversely pumped laser (Eq. (33)). In the former the growth rate decreases as $\gamma^{-11/4}$ whereas in the latter it decreases as $\gamma^{-3/4}$. This makes the longitudinal pumped TM laser very unattractive for producing ultrashort wavelengths radiation with high γ electron beam generators, a fact already mentioned earlier in this section.

Now, let us consider the longitudinally pumped TM system

operating near cutoff of one of the (m,ν) modes of the cylindrical waveguide, as discussed earlier. Transforming $\Gamma(\omega\simeq\omega_c)$ of Eq. (43) into the laboratory frame of reference gives

$$\Gamma_L(\omega \simeq \omega_c) = \left[\frac{\omega_{po}\ell_L}{32\pi\beta c\gamma^{3/2}}\right]^{1/2}\left(\frac{q}{m_o}\frac{E_{zL}}{\gamma\beta c}\right) \tag{46}$$

Observe the $\gamma^{-7/4}$ dependence of Γ. To excite the instability, one must adjust the pump frequency so that $\omega_3\simeq\omega_c$. This requires, in the laboratory frame of reference, that

$$\omega_{3L} = \omega_c \simeq 2\pi\beta c\gamma/\ell_L. \tag{47}$$

Although the growth rate can be reasonably large (for not too large values of γ), we stress that the frequency of the generated electromagnetic wave ($\simeq\omega_c$) is relatively low (there is no γ^2 frequency multiplication). For example, in a waveguide of 0.5cm radius operating in the (0,1) mode, $\omega_{3L}/2\pi\simeq 23$GHz; in the (3,3) mode $\omega_{3L}/2\pi\simeq 113$GHz. Nonetheless, the system could find application in the generation of large fluxes in the millimeter wavelength range.

V. DISCUSSION

On previous pages we dealt with Raman-like scattering from dense, relativistic electron beams driven parametrically by means of electric field pumps. When the pump electric field is oriented perpendicular to the direction of beam propagation, the physical situation is much the same as for "magnetic wigglers" treated exhaustively in earlier works:[17-20] in both systems, axial electron bunching necessary for wave amplification comes about via the radiation pressure force (i.e. the ponderomotive force); the electrical pump field $E_\perp$ in the electrically excited system plays the same role as the magnetic pump field $B_\perp=E_\perp/c$ in the magnetic wig-

gler system.

When the relevant electric field component of the pump wave is oriented along the direction of beam propagation, axial electron bunching is induced directly by the axial electric field, and there is no need for the intervention of the ponderomotive force. Two types of parametric interactions are distinguished. The one involves coupling of the slow and fast space charge waves propagating on the beam, and is treated in Section III. The other involves the coupling of the slow space charge wave and a TM electromagnetic wave supported by the waveguide structure. This problem is discussed in Section IV. In these sections the discussion is restricted to static pumps ($\omega_{1L}=0$) only; the general analysis, however, given in Section II is valid for pumps of any frequency.

The results of the computations are summarized in Table I in which we list the growth rates and frequencies of the backscattered waves for each interaction. Let us compare the three. The transversely driven system (top of Table I) and the longitudinally driven TM mode interaction (third from the top of Table I) can be excited with an almost limitless choice of pump periodicities, the only limitation being imposed by the selection rules 17 and waveguide cutoff, which require that, in the notation of previous sections, the pump wavenumber k_{1L} satisfy the inequality,

$$k_{1L}c > \left[\omega_c(\gamma^2-1)^{-1/2} + \omega_{pL}/\beta\right] . \qquad (48)$$

As a result, the maximum achievable backscattered frequencies ω_{3L} (see Table I) can be very large. On the other hand, in the two-space charge wave process (second from the top of Table I) the pump periodicity is limited by the fact that in the beam frame

$\omega_1 \leq 2\omega_p$. This imposes the condition that, in the laboratory frame,

$$k_{1L} \leq 2\omega_{pL}/\gamma\beta c \qquad (49)$$

Consequently, the maximum frequency of the backscattered wave ω_{3L} (see Table I) that can be achieved is determined by beam density.

Let us now turn to the growth rates. The two-space charge wave process can have a considerably larger growth rate than the transversely pumped free electron laser system. This advantage is, however, offset somewhat by the following consideration. The transeversely pumped system generates a fast backscattered electromagnetic wave whose phase velocity within the waveguide structure is greater than, or equal to c. Thus, the wave can be coupled out of the interaction region efficiently by standard optical methods. The two-space charge wave interaction, on the other hand, gives rise to a wave whose velocity is typically the beam velocity v_o and is therefore a little slower than c. To extract the electromagnetic energy efficiently may require a suitable slow wave circuit, as for example a dielectric loaded waveguide provided with holes, or a continuous axial slot, which couples the beam loaded guide to the extraction circuit.

The longitudinally driven TM mode system (third from the top of Table I) exhibits a growth rate which is smaller than the growth rate of the transversely pumped laser in the ratio $\sim(\ell_L/\ell_c)(\beta\gamma^2)^{-1}$. Here $\ell_L=2\pi k_{1L}$ is the periodicity of the pump and $\ell_c=2\pi c/\omega_c$ is the cutoff wavelength for the waveguide mode in question. Since $\ell_L \lesssim \ell_c$ and γ is typically 1 to 10, the growth rate of the longitudinally driven wave generator is considerably less than that of the transversely pumped laser. The exception is to

operate near the cutoff frequency (bottom line of Table I) where the growth rate is once again sizable.

In conclusion, then, we see that the most promising systems are the two listed at the top of Table I: the transversely driven laser, and one employing two interacting space charge waves. We have not addressed the question of how to generate static, periodic, transverse or longitudinal electric field pumps of sufficient strength. This problem is discussed elsewhere.[13]

ACKNOWLEDGMENTS

This work is supported in part by the U.S. Air Force Office of Scientific Research (Grant AFOSR77-3143B), and in part by the National Science Foundation (Grant ENG79-07047).

REFERENCES

1. J.M.J. Madey, J. Appl. Phys. 42, 1906 (1971); J.M.J. Madey, H.A. Schwettmann, and W.M. Fairbank, IEEE Trans. Nucl. Sci. NS-20, 980 (1973).
2. L.R. Elias, W.M. Fairbank, J.M.J. Madey, H.A. Schwettman, and T.I. Smith, Phys. Rev. Lett. 36, 717 (1976).
3. D.A.G. Deacon, L.R. Elias, J.M.J. Madey, G.J. Ramian, H.A. Schwettman, and T.I. Smith, Phys. Rev. Lett. 38, 892 (1977).
4. V.L. Granatstein, S.P. Schlesinger, M. Herndon, R.K. Parker, and J.A. Pasour, Appl. Phys. Lett. 30, 384 (1977).
5. T.C. Marshall, S. Talmadge, and P. Efthimion, Appl. Phys. Lett. 31, 320 (1977).
6. R.K. Parker, W.M. Black, K. Tobin, M. Herndon, and V.L. Granatstein, Bull. Am. Phys. Soc. 23, 863 (1978).
7. R.M. Gildenbach, Ph.D. thesis Columbia University, 1978.
8. D.B. McDermott, T.C. Marshall, S.P. Schlesinger, R.K. Parker, and V.L. Granatstein, Phys. Rev. Lett. 41, 1368 (1978).
9. R.M. Gildenbach, T.C. Marshall, and S.P. Schlesinger, Phys. of Fluids 22, 971 (1979).
10. R.M. Gildenbach, T.C. Marshall, and S.P. Schlesinger, Phys. of Fluids 22, 1219 (1979).
11. G. Bekefi and R.E. Shefer, Proceedings of the 1979 IEEE International Conference on Plasma Science Montreal 1979, page 12.
12. R.E. Shefer and G. Bekefi, Proceedings of the 1979 IEEE International Conference on Plasma Science Montreal 1979, page 13.

13. G. Bekefi and R.E. Shefer, J. Appl. Phys. 50, 5158 (1979).

14. The scattering mechanism discussed in Section IV of this paper has also been analyzed via the Vlasov equation approach by A. Gover. It is to be published in the Proceedings of Free Electron Lasers, Telluride, Colorado 1979. (Private Communication 1979.)

15. H. Motz, J. Appl. Phys. 22, 527 (1951).

16. V. P. Sukhatme and P.W. Wolff, J. Appl. Phys. 44, 2331 (1973); IEEE J. Quantum Electron QE-10, 870 (1974).

17. A. Hasegawa, K. Mima, P.A. Sprangle, H.H. Szu, and V.L. Granatstein, Appl. Phys. Lett. 29, 542 (1976).

18. P.A. Sprangle and V.L. Granatstein, Appl. Phys. Lett. 25, 377 (1974); P.A. Sprangle, V.L. Granatstein, and L. Baker, Phys. Rev. A12, 1697 (1975); P.A. Sprangle and A. T. Drobot, Naval Research Laboratory Report 3587, 1978.

19. P.A. Sprangle, R.A. Smith, and V.L. Granatstein, Naval Research Laboratory Report No. 3911, 1978.

20. N.M. Kroll and W.A. McMullin, Phys. Rev. A17, 300 (1978).

21. Y.W. Chan, Phys. Rev. Lett. 42, 92 (1979).

22. W.P. Allis, S.J. Buchsbaum, and A. Bers, Waves in Anisotropic Plasmas (M.I.T. Press, 1963).

23. A.W. Trivelpiece and R.W. Gould, J. Appl. Phys. 30, 1784 (1959).

24. E.A. Frieman, J. Math. Phys. (N.Y.) 4, 410 (1963); Physica (Utrecht) 31, 693 (1965).

25. C.K. Birdsall, Proc. IRE 42, 1628 (1954).

26. W.H. Louisell and C.F. Quate, Proc. IRE 46, 707, (1958).

Table I. Stimulated Scattering in Static Transverse and Longitudinal Electric Fields in the Laboratory (L) Frame. The temporal growth rate is given by $\Gamma_L = G_L(qE_L/m_o v_o \gamma)$; $\beta = v_o/c$; $\gamma = (1-\beta^2)^{-1/2}$; $\omega_{po} = (N_L q^2/m_o \varepsilon_o)^{1/2}$; $\omega_{co} = p_{m\nu} c/a$. F is shown in Fig. 7.

Pump Wave (1)	Waves (2) and (3)	Frequency of backscattered wave ω_{s_L}(rad-sec^{-2})	Temporal growth rate factor G_L
Transverse $E_\perp$ or $B_\perp$	Space charge plus TE or TM wave	$\dfrac{2\pi v_o (1+\beta)\gamma^2}{\ell_L}$	$\sqrt{\dfrac{\gamma^{1/2}\omega_{po}\ell_L}{32\pi v_o}}$
Longitudinal E_z	Two space charge waves	$\dfrac{2\pi v_o \gamma^2}{\ell_L} F$	$\dfrac{3}{8}$ (maximum)
Longitudinal E_z	Space charge plus TM wave	$\dfrac{2\pi v_o (1+\beta)\gamma^2}{\ell_L} >> \omega_c$	$\sqrt{\dfrac{(1+\beta^2)\omega_{po}\omega_{co}^2\ell_L^3}{512\pi^3\gamma^{7/2}v_o^3}}$
		ω_c	$\sqrt{\dfrac{\omega_{po}\ell_L}{32\pi\gamma^{3/2}v_o}}$

FIGURE CAPTIONS

Fig. 1. Schematic dispersion diagrams illustrating the coupling between a static pump wave (1), a slow space charge wave (2), and a fast space charge wave (3), as observed in the beam frame (top) and the laboratory frame (bottom). For clarity, the two figures are drawn to different scales.

Fig. 2. Schematic dispersion diagrams illustrating the coupling between a static pump wave (1), a slow space charge wave (2), and a TM mode (3) of the waveguide, as observed in the beam frame (top), and the laboratory frame (bottom). For clarity, the two figures are drawn to different scales.

Fig. 3. Geometry of the electron beam traveling through a cylindrical waveguide and confined by a strong, axial magnetic field.

Fig. 4. Frequency relationships between the three waves of Fig. 1 required by the selection rules 17, as a function of the beam parameter b. The dashed lines refer to wave 2, the solid lines to wave 3.

Fig. 5. The temporal growth rate parameter G of Eqs. (19) and (20) (in the beam frame) for the backscattered space charge wave, as a function of the beam parameter b, for different values of the pump frequency ω_1.

Fig. 6. The Landau damping limit D of Eq. (29) for the backscattered space charge wave, as a function of the beam parameter b,

for different values of the pump frequency ω_1.

Fig. 7. The dimensionless quantity $F=\omega_{3L}/k_{1L}\gamma^2\beta c$ (in the laboratory frame) as a function of the beam parameter b_L for different values of the pump frequency ω_1.

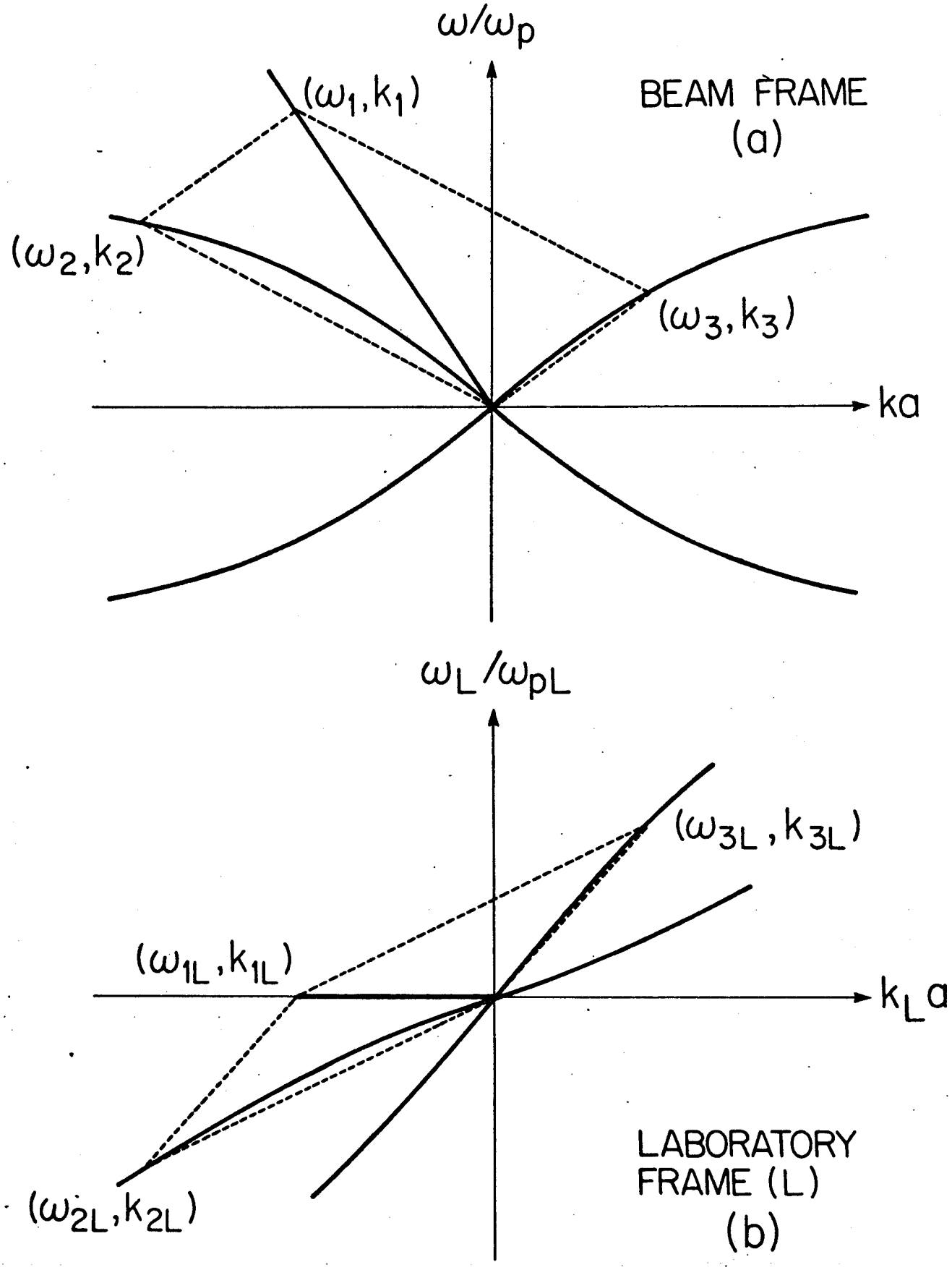
ω/ω_p
(ω_1, k_1)
BEAM FRAME
(a)
(ω_2, k_2)
(ω_3, k_3)
ka
ω_L/ω_{pL}
(ω_{3L}, k_{3L})
(ω_{1L}, k_{1L})
$k_L a$
LABORATORY
FRAME (L)
(b)
(ω_{2L}, k_{2L})

Fig. 1
Bekefi

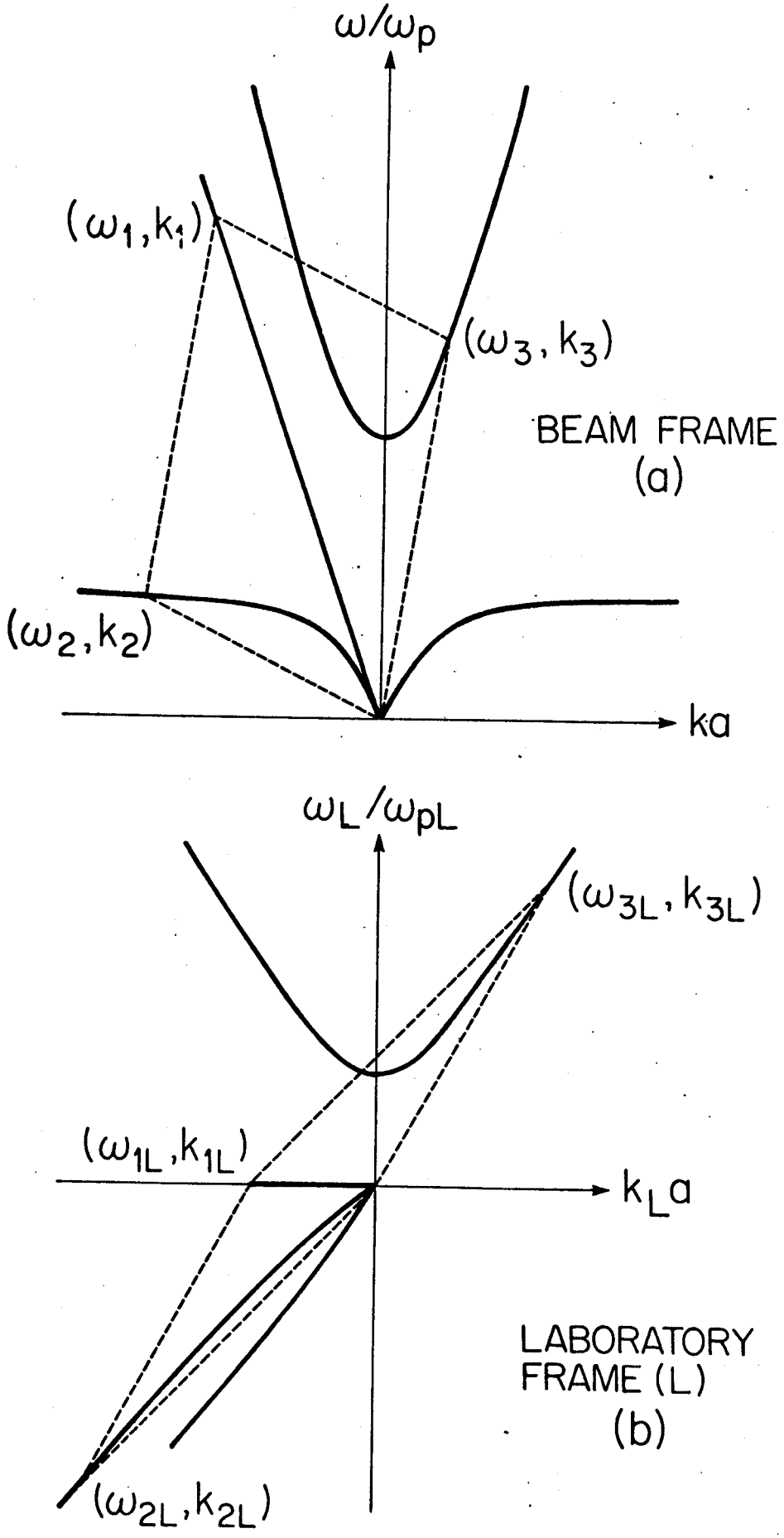
ω/ωp
(ω1,k1)
(ω3,k3)
BEAM FRAME
(a)
(ω2,k2)
ka
ωL/ωpL
(ω3L,k3L)
(ω1L,k1L)
kLa
LABORATORY
FRAME (L)
(b)
(ω2L,k2L)

Fig. 2
Bekefi

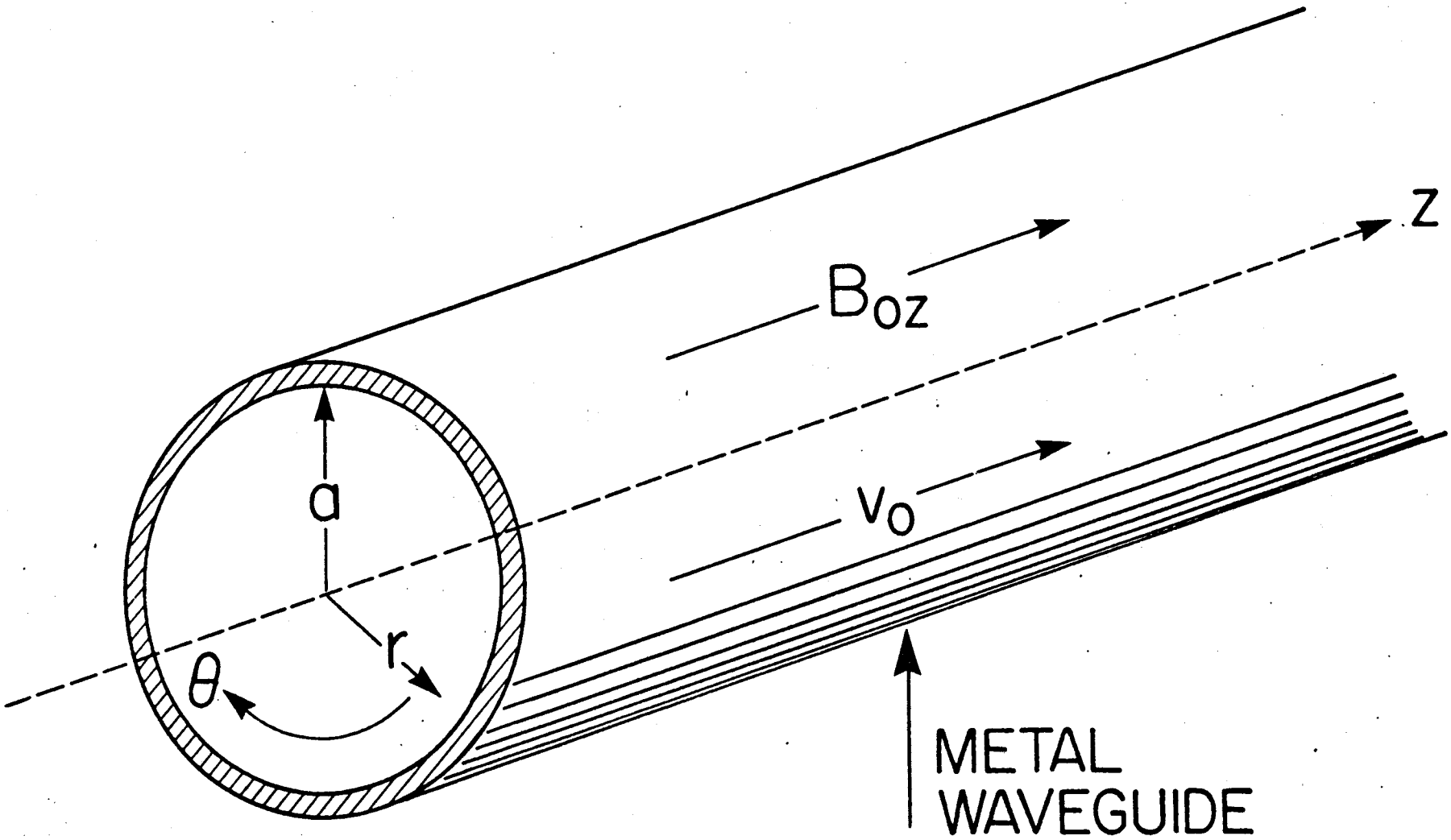

Fig. 3
Bekefi

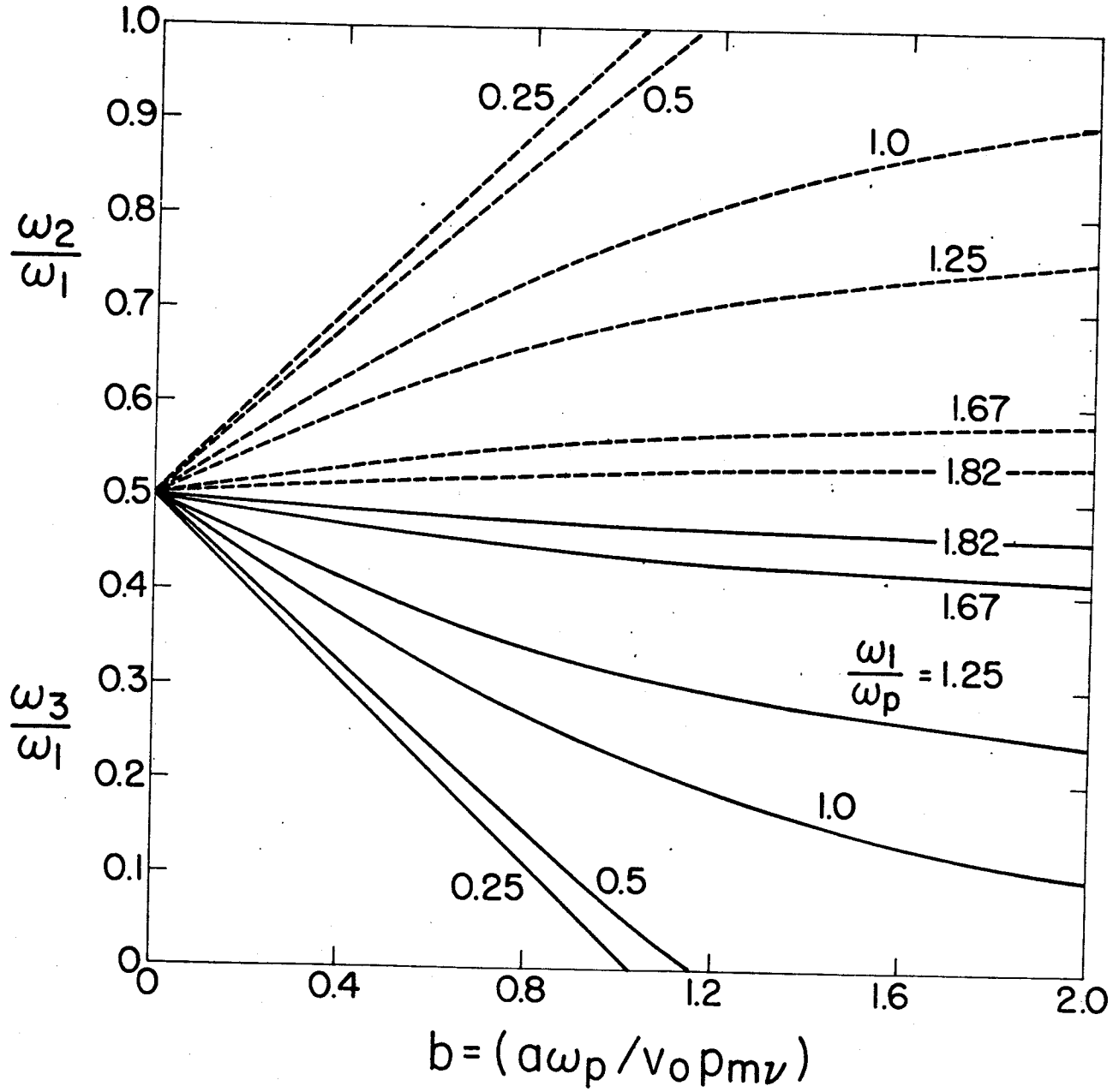
1.0
0.9
0.8
0.7
0.6
0.5
0.4
0.3
0.2
0.1
0
0
0.4
0.8
1.2
1.6
2.0
ω2/ω1
ω3/ω1
0.25
0.5
1.0
1.25
1.67
1.82
1.82
1.67
ω1/ωp = 1.25
1.0
0.25
0.5
b = (aωp/v0pmν)

Fig. 4
Bekefi

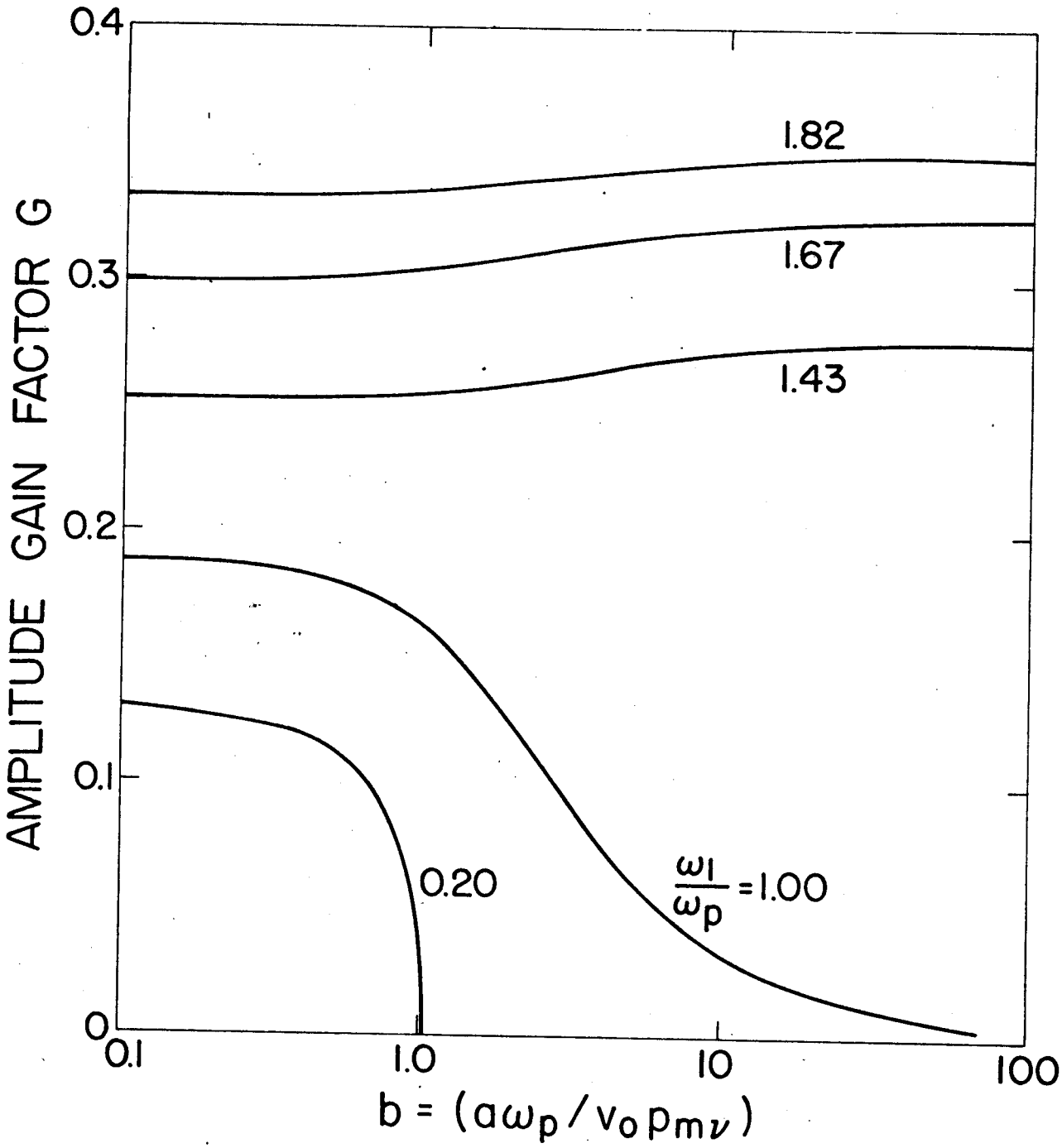
0.4
0.3
0.2
0.1
0
AMPLITUDE GAIN FACTOR G
1.82
1.67
1.43
0.20
ω1/ωp =1.00
0.1
1.0
10
100
b = (aωp/v0pmν)

Fig. 5
Bekefi

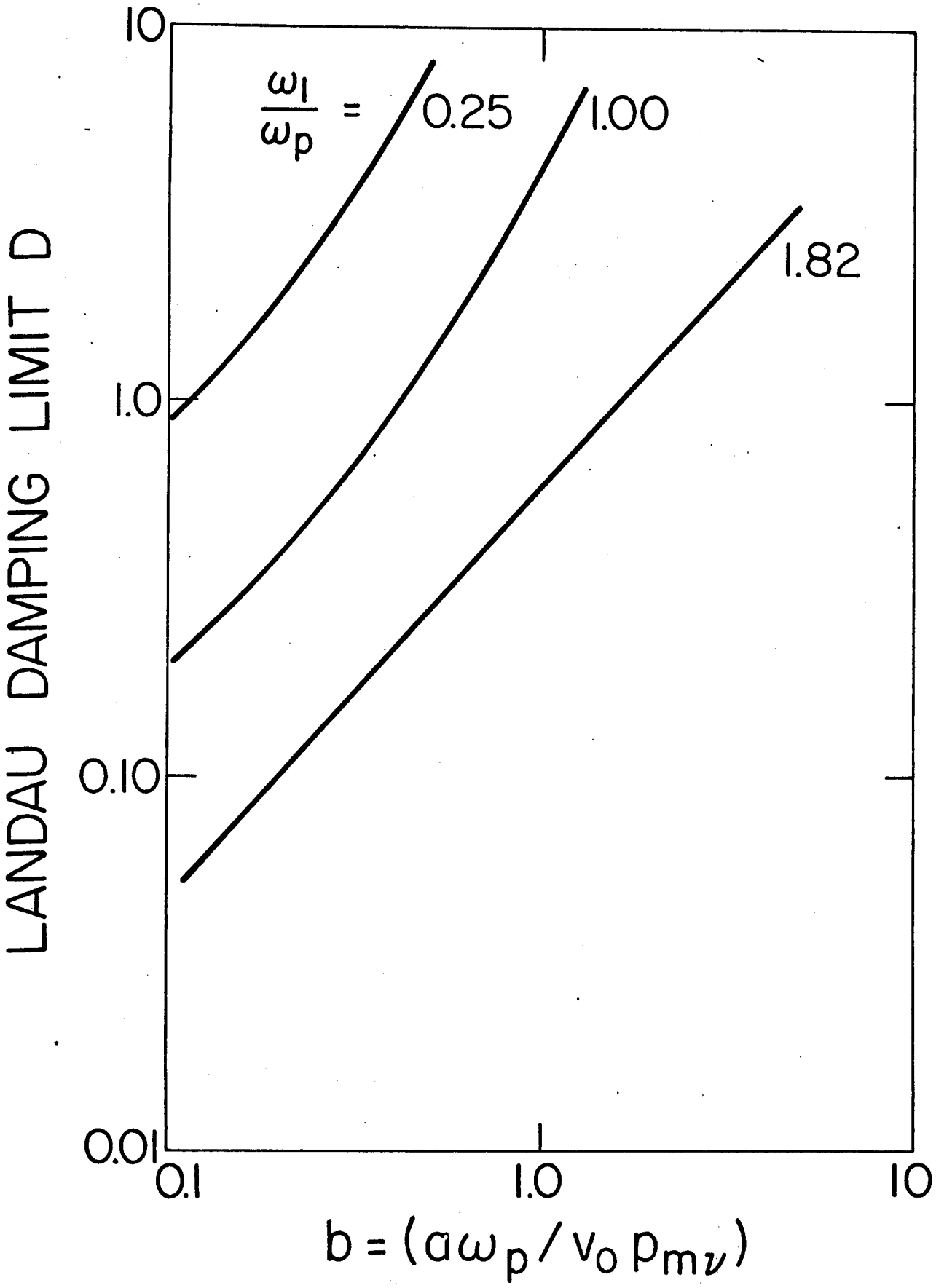
LANDAU DAMPING LIMIT D
10
1.0
0.10
0.01
0.1
1.0
10
$\frac{\omega_1}{\omega_p}$ =
0.25
1.00
1.82
$b = (a\omega_p / v_0 p_{m\nu})$

Fig. 6
Bekefi

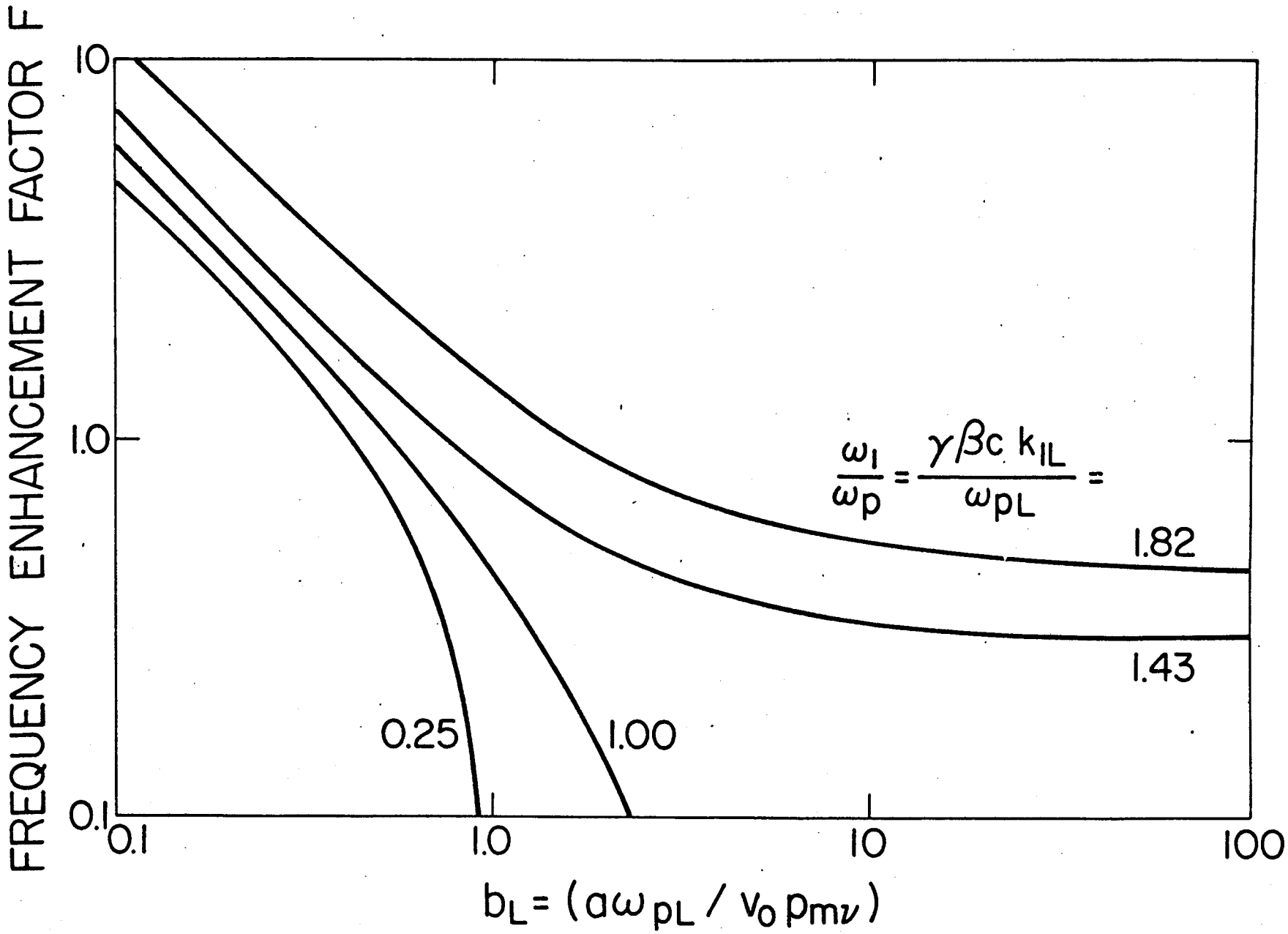
FREQUENCY ENHANCEMENT FACTOR F
10
1.0
0.1
0.1
1.0
10
100
$b_L = (a\omega_{pL} / v_0 p m\nu)$
$\frac{\omega_I}{\omega_p} = \frac{\gamma\beta c\, k_{IL}}{\omega_{pL}} =$
1.82
1.43
1.00
0.25

Fig. 7
Bekefi